Developments in Environmental Science, Volume 5
D. Sarkar, R. Datta and R. Hannigan (Editors)

ISSN: 1474-8177/DOI:10.1016/S1474-8177(07)05019-X

Chapter 19

Using GIS to display complex soil salinity patterns in an inland salt marsh

Matthew Grunstra and O.W. Van Auken

Abstract

Inland salt marshes are found near salt lakes and desert springs in areas of high evaporation and low precipitation. Spatial and seasonal fluctuations of the soil salinity levels are assumed to be associated with local climate. However, topography complicates the general soil salinity patterns attributed to climate. To better demonstrate and display these spatial and temporal relationships, soil salinity data were gathered over a ten-month period and then examined with a geographic information system software package. A variety of surface contour plots can be generated depending on the software used, the interpolation method, and the input variables chosen. To demonstrate some of this variation, surface plots were interpolated using the inverse distance weighted method in ArcView 3.3 and the ordinary kriging method in ArcGIS 8. Various methods and settings should be examined to create the clearest interpolated surface to present the collected data. Using the same data, ordinary kriging generated a gradual, smooth surface while the overall quality of the inverse distance weighted surface was irregular. The ordinary kriging method produced mean error and root-mean-square error statistics closer to zero indicating it would generally yield a better estimation of the soil salinity. The surfaces generated showed some seasonal fluctuation in soil salinity but spatial changes were more distinct. The low-elevation areas in the center of the salt marsh had low levels of soil salinity while the marsh edges at slightly higher elevations had increased levels of soil salinity. The spatial patterns of soil salinity appear to depend on seasonality, specifically rainfall and plant activity and the amount of water present in the salt marsh. However, local surface anomalies can mask these patterns. Through the use of global information systems (GIS) and interpolation some of the masking effects can be reduced revealing the underlying patterns.

19.1. Introduction

Geographical information systems (GIS) and global positioning systems (GPS) provide new ways to investigate and display areas both spatially and temporally. The surface contour plot is a tool readily available with the emergence of cheaper GIS software. A surface contour plot allows a limited point dataset to be expanded to display estimated values at any point within a study area, thereby possibly reducing the amount and expense of sampling.

There are numerous interpolation methods available for the creation of these surface contours (Lam, 1983; Isaaks and Srivastava, 1989; Burrough and McDonnell, 1998). Each of these individual interpolation methods allow the user to modify characteristics and input variables that can yield large variations in the output surface. As of yet there is no universally accepted systematic approach to method selection. This chapter will demonstrate different output surfaces created using two of the more common interpolation techniques, Inverse Distance Weighted (IDW) and Ordinary Kriging (Franzen and Peck, 1995; Weisz et al., 1995). It will also demonstrate how these surfaces can be applied to field research by examining the spatial and temporal fluctuations of soil salinity levels in an inland salt marsh.

The IDW method is a local deterministic interpolation technique (ESRI, 1999; Ormsby and Alvi, 1999; Johnston et al., 2001). A local technique calculates the estimated values for the entire study area based on small spatial areas or neighborhoods. The IDW method is an exact interpolator which predicts a value at a sample location that is equal to the measured value in the dataset (ESRI, 1999; Johnston et al., 2001). The calculations used with this procedure are based on the principle that each data point has a local influence that is reduced with distance (ESRI, 1999; Ormsby and Alvi, 1999; Johnston et al., 2001). The IDW method produces accurate surface interpolation as long as a regularly distributed sampling pattern is used in data collection (ESRI, 1999, 2000; Ormsby and Alvi, 1999; Johnston et al., 2001). Low concentration or an uneven distribution in the sampling points often produces sharp peaks or troughs in the output surface (Ormsby and Alvi, 1999; ESRI, 2000; Johnston et al., 2001).

The ArcGIS 8 software allows the use of the geostatistical interpolation method of ordinary kriging to create surface contour plots. Kriging has theoretical advantages over the IDW method because it is a geostatistical technique which is based on the principle that direction or distance between points reflects a spatial correlation that can explain the variation of the surface (Isaaks and Srivastava, 1989; Burrough and McDonnell, 1998; ESRI, 2000; Johnston et al., 2001; ESRI, 2003). Ordinary kriging is based on the principle that direction or distance between points reflects a spatial correlation that can explain the variation of the surface (ESRI, 2000; Johnston et al., 2001).

The Geostatistical Analyst extension in the ArcGIS 8.0 software also allows cross-validation of the prediction errors, which serves as a diagnostic tool to evaluate the surface plot generated (Johnston et al., 2001). Cross-validation uses all of the dataset to estimate the model and then it removes each data location, one point at a time, and predicts the associated data value (Johnston et al., 2001). The prediction error statistics include a mean error, root-mean-square error, average standard error, and the root-mean-square standardized error (Johnston et al., 2001).

Many studies have compared the performance of these two methods using cross-validation techniques and generation of error statistics (Warrick et al., 1988; Laslett et al., 1987; Wollenhaupt et al., 1994; Gotway et al., 1996; Kravchenko and Bullock, 1999; Brodsky et al., 2001; Mueller et al. 2001; Jones et al., 2003; Kravchenko, 2003; Mueller et al., 2004). Several studies found kriging to produce lower root-mean-square errors than the IDW method for their data (Lefohn et al., 1987; Kravchenko and Bullock, 1999; Bekele et al., 2003). Others authors have indicated IDW as a more suitable method with the IDW method generating a lower root-mean-square error than the kriging method when investigating soil properties in western Australia (Robinson and Metternicht, 2005). Some studies used other generated error statistics such as mean error, mean absolute error, and error standard deviation (Phillips et al., 1997) or log mean squared error (Zimmerman et al., 1999) to evaluate performance between the different methods. Most often sampling location, spatial correlation and grid scale were found to influence the optimal method (Bucher and Vckovski, 1995; Gotway et al., 1996; Brodsky et al., 2001; Dille et al., 2003; Jones et al., 2003; Kravchenko, 2003; Mueller et al., 2004). The varied results in each of these studies indicate careful consideration should be employed when determining the interpolation method and settings to be used with a given dataset.

Many studies of soil salinity, vegetation and salt marshes have incorporated GIS into their analysis or presentation of their data. GIS interpolations have been used to determine the spatial dynamics of soil salinity in arid and in semi-arid conditions (Jordan et al., 2004) as well as to determine the temporal and spatial variability of soil salinity in a coastal saline field (Shi et al., 2005) and a cotton field irrigated with low-quality water (Cetin and Kirda, 2003). Recent and subfossil vegetation data was imported into a GIS software package and used to investigate and determine long-term salt marsh vegetation dynamics on Frisian barrier islands off the coast of Germany (Freund et al., 2003). GIS combined with aerial photography has indicated the broad distribution of the vegetational patterns in a Georgia tidal salt marsh were due to salinity (Higinbotham et al., 2004).

Saline marshes are of two general types, marine and inland, and occur in many different geographical areas worldwide (Odum, 1988). Marine marshes are found along large bodies of saltwater, and are usually considered coastal salt marshes (Chapman, 1974). Inland salt marshes typically occur in desert areas usually without a large body of water nearby. Inland marshes develop within high-evaporation basins, usually next to inland saline lakes, and lowlands associated with desert springs (Odum, 1988). This is due to the high rate of evaporation and low level of precipitation in these desert ecosystems. The level of salts and the kind of salts found in the soil vary in both time and location (Borchert, 1971; Ungar, 1974). This is due to the amount of precipitation, timing of the precipitation in the system and the underlying rock type (Brune, 1981).

The Diamond Y Spring is located on a 6.1 km^2 nature preserve owned by the Nature Conservancy of Texas located approximately 16 km north of Fort Stockton, Texas (Fig. 19.1). The Diamond Y Spring is the last major spring still flowing in Pecos County, Texas (Veni, 1991). The Diamond Y Spring Preserve protects six federally endangered or threatened species. Included are the Puzzle Sunflower (*Helianthus paradoxus*), Leon Springs Pupfish (*Cyprinondon bovinus*), Pecos Gambusia (*Gambusia nobilus*), Diamond Y Spring snail (*Tryonia adamantia*), Gonzalez Spring Snail (*Tryonia stocktonensis*), and Pecos Assiminea snail (*Assiminea pecos*) (McDonald, 1999; Bush and Van Auken, 2004; Van Auken et al., 2007).

The types of soil, water chemistry, as well as, the plant communities present are all indicators that the low elevation area at the Diamond Y Spring Preserve is a salt marsh (Chapman, 1974; TPWD, 2003). Soils in the study area are composed mainly of three associations: the Balmorhea, Orla, and Lozier (Rives, 1980; Grunstra, 2002) (Fig. 19.1). These soils are found in specific areas of the Diamond Y Spring Preserve due to elevation and soil water. Balmorhea soils tend to be deep (>152 cm) moderately saline and poorly drained often occupying lower elevation areas in and around spring fed marshes where they are usually anaerobic due to continuous saturation (Fig. 19.1) (Rives, 1980; Lavelle and Spain, 2001; Bush, 2002; Grunstra, 2002). Balmorhea soils are Mollisols and are classified as fine-silty, thermic Cumulic Haplaquolls (Schoeneberger et al., 1998). These soils are usually gray silt loam containing fine concretions of calcium carbonate (Rives, 1980; Lavelle and Spain, 2001). Orla soils are Aridisols and are classified as fine-loamy, gypsic, thermic Typic Gypsiorthids (Schoeneberger et al., 1998). Orla soils tend to be located in

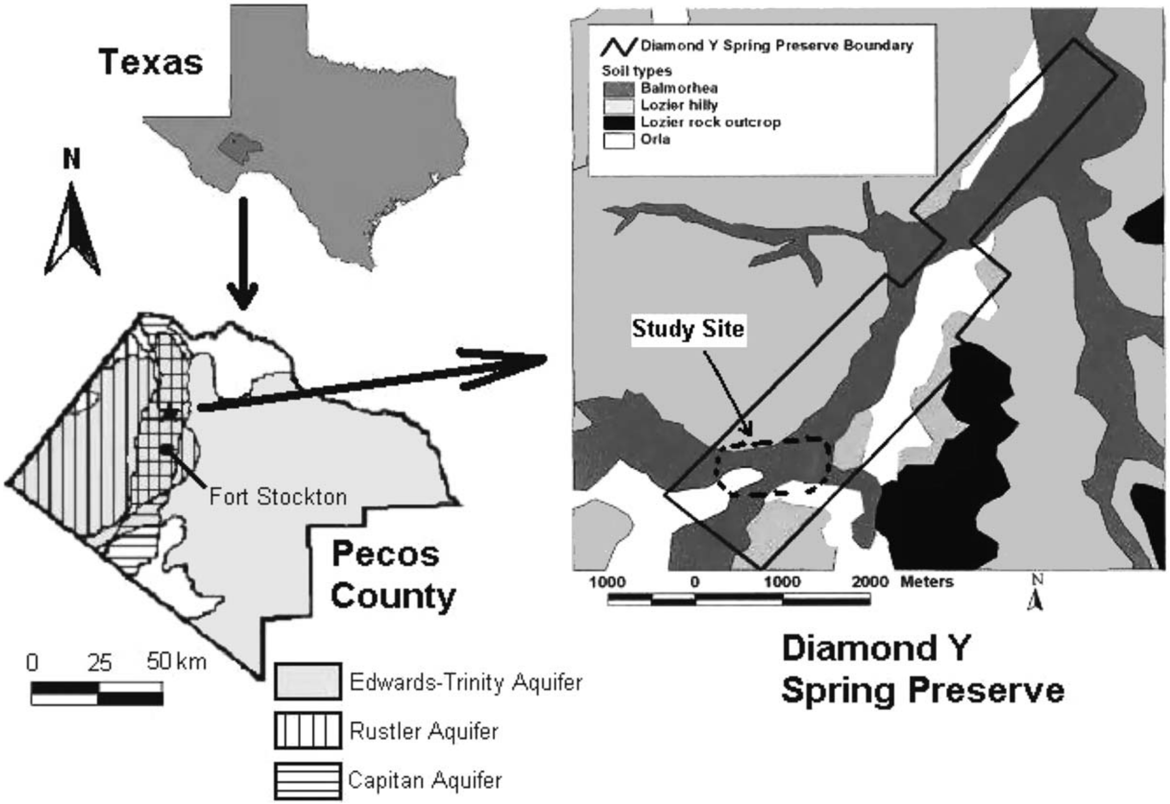

Figure 19.1. Pecos County is located in west Texas, USA. The major aquifers underlying the Fort Stockton area and Pecos County, Texas include the Edwards-Trinity, Rustler, and Capitan Reef. Soil types present in the area of the Diamond Y Spring Preserve include Balmorhea, Orla, and Lozier association soils (Rives, 1980).

the low to medium elevations of the study area, usually higher in elevation than the Balmorhea soils and above the salt marsh (Fig. 19.1) (Grunstra, 2002). Gypsum and loam comprises 40–80% of the composition of these soils giving them a moderately alkaline pH, moderate permeability, and a low water holding capacity (Rives, 1980; Schoeneberger et al., 1998; Lavelle and Spain, 2001). Lozier soils occupy the higher elevations surrounding the salt marsh, above the Orla soils, lying on the limestone outcrops (Fig. 19.1) (Grunstra, 2002). Lozier series soils are Aridsols and are classified as loamy-skeletal, carbonatic, thermic Lithic Calciorthids (Schoeneberger et al., 1998). Lozier soil is well drained, shallow, moderately alkaline and characterized as gravely and stoney, light brownish gray in color with high limestone content (Rives, 1980; Lavelle and Spain, 2001).

There have been a number of studies done on the area hydrology but nothing specific to the Diamond Y Spring Preserve (Boghici, 1997). The general physiographic setting of the Diamond Y Spring Preserve is a semi-arid karst terrain with an average annual precipitation of 33 cm year^{-1} and an evaporative rate of 204 cm year^{-1} (Fig. 19.2) (Larkin and Bomar, 1983). The aquifers underlying the area are: the Capitan Reef Complex, Rustler, and Edwards-Trinity (Fig. 19.1).

The Capitan Limestone formation lies approximately 1200 m below the Diamond Y Spring Preserve and generally contains highly mineralized calcium–magnesium bicarbonate water with dissolved-solids concentrations that range from 850 to 2500 mg l^{-1} (Veni, 1991; USGS, 2002). The Rustler aquifer lies in the carbonates and evaporites of the Rustler Formation at a depth of approximately 220 m under the Diamond Y Spring Preserve (Veni, 1991) and uniformly yields water high in calcium and low in bicarbonate (Small and Ozuna, 1993; Boghici, 1997). Total dissolved solids range from 1500 to 80,000 mg l^{-1} (Veni, 1991). The Edwards-Trinity aquifer is found beneath most of Pecos County and covers areas underlain by both the Capitan Reef Complex and Rustler aquifers (Fig. 19.1). The depth of the Edwards-Trinity aquifer under the Diamond Y Spring Preserve is approximately 85 m. The Edwards-Trinity aquifer water is dominated by sulfate and chloride with high concentrations of sodium, calcium, and magnesium cations (Veni, 1991; USGS, 2002). In Pecos county, Edwards-Trinity aquifer water can be fresh to brackish containing less than 1500 mg l^{-1} total dissolved solids or with total dissolved solids up to 80,000 mg l^{-1} due to mixing with Rustler water (Veni, 1991; Boghici, 1997).

The aquifer that feeds the Diamond Y Spring is a point of slight contention. In 1991, Veni suggested it was the Edwards-Trinity aquifer. However, in 1997, Boghici suggested that the Rustler aquifer feeds the

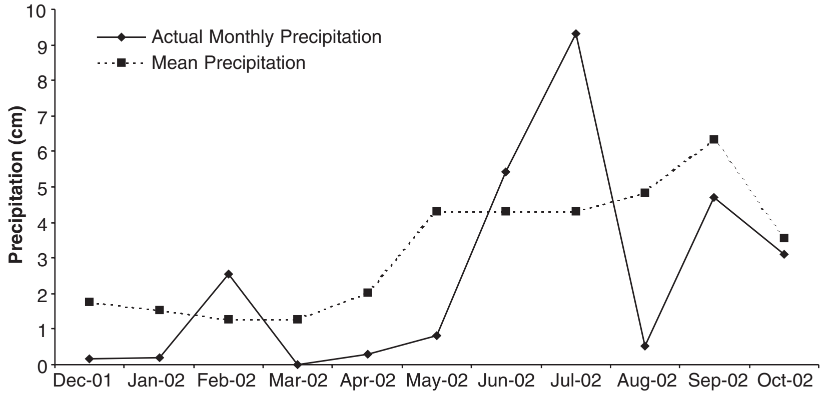

Figure 19.2. Total monthly precipitation data from December 2001 to October 2002. The values are plotted for the center of the months. The solid line is the actual monthly precipitation reported from Fort Stockton, Texas. The mean precipitation data are based on 1231 months from 1859 to 1987 (NCDC, 2002).

preserve. In either case, the water has been found to be dominated by a sodium–chloride–sulfate chemistry with moderate amounts of calcium and magnesium (Veni, 1991; USGS, 2002). The Diamond Y Spring is located approximately 1000 m southwest of the current study site flowing into the drainage area where it joins with Leon Creek flowing from the west creating the salt marsh. The water drains eastward mostly through subsurface flow out of the marsh approximately 25 km to the Pecos River. The surface flow is ephemeral due to the low rainfall and high-evaporative rate (Van Auken and Bush, 1998; Grunstra, 2002; Hart, 2002).

The plant communities located within the salt marsh are in fairly distinct locations across the marsh landscape (Grunstra, 2002; Grunstra and Van Auken, 2007; Van Auken et al., 2007). This distribution may be due to the different species specific water requirements, salt tolerance, or ability to out-compete rivals in the differing salinity levels of the soil (Chapman, 1974; Niering and Warren, 1980; Bertness, 1991; Van Auken and Bush, 1998; Bush, 2002; Grunstra and Van Auken, 2007; Van Auken et al., 2007). Surrounding the marsh at a slightly higher elevation are *Prosopis glandulosa* woodlands (Van Auken and Bush, 1998). Slightly lower within the marsh are three distinct grassland communities. The *Sporobolus airoides* grassland is slightly higher and drier than the *Distichlis spicata* community that is usually located in areas that are flooded for at least part of the year. In the deepest soils of the central areas of the marsh in soils that are usually flooded year round is the *Schoenoplectus Americana* community.

To gain a greater understanding of the distribution of the soil salinity throughout the marsh and its possible relationship with the salt marsh vegetation, soil salinity data were gathered. The point data were then placed into a GIS software package in which a surface contour plot was generated. The surface contour plot interpolated values to fill in the study area and provide a representative overview of the soil salinity levels throughout the salt marsh. Different geographic information system software, interpolation methods, and input variables will generate visually different surface contour plots and should be investigated for the creation of the most useful interpolated surface of the data.

19.2. Methods

The borders of the study area were designated on the northern, western, and eastern edges by fencing that allows controlled grazing on the marsh. A sharp change in elevation out of the lowland and into the slightly higher elevation of the surrounding limestone outcropping set the southern limit of the study area. A grid pattern of observation points was chosen to cover the study area based on an existing pattern of observation wells located in the southwestern corner of the marsh (Bush, 2002). The grid pattern used in the present study was expanded to a larger scale in order to increase the size of the study area and encompass a larger area of the salt marsh. The grid pattern consisted of 7 transects with a total of 87 observation points (Fig. 19.3).

A GeoExplorer III GPS receiver unit along with a Beacon-on-a-Belt both manufactured by Trimble were used to map the study area and the 87 observation points. For the observation points, a mean of ten measurements per position were collected which helps to increase the precision of the location data collected by increasing the size of the sample set. The position mode was set to collect 3D data using a minimum of four satellites. The majority of the GPS measurements for each location were collected using six to eight satellites while only three locations used five satellites. The elevation mask was set for twenty degrees to reduce the amount of ionosphere noise, which is above the recommended minimum setting of fifteen degrees (Trimble, 1999). The signal-to-noise ratio mask was set at ten to ensure acceptance of only strong satellite signals and reduce noise distortion. The Position Dilution of Precision mask was set at five to ensure the use of an even geometric distribution of satellites (Trimble, 2001).

Trimble's Beacon-on-a-Belt allowed the data to be real time differentially corrected. Differential correction calculates the errors associated

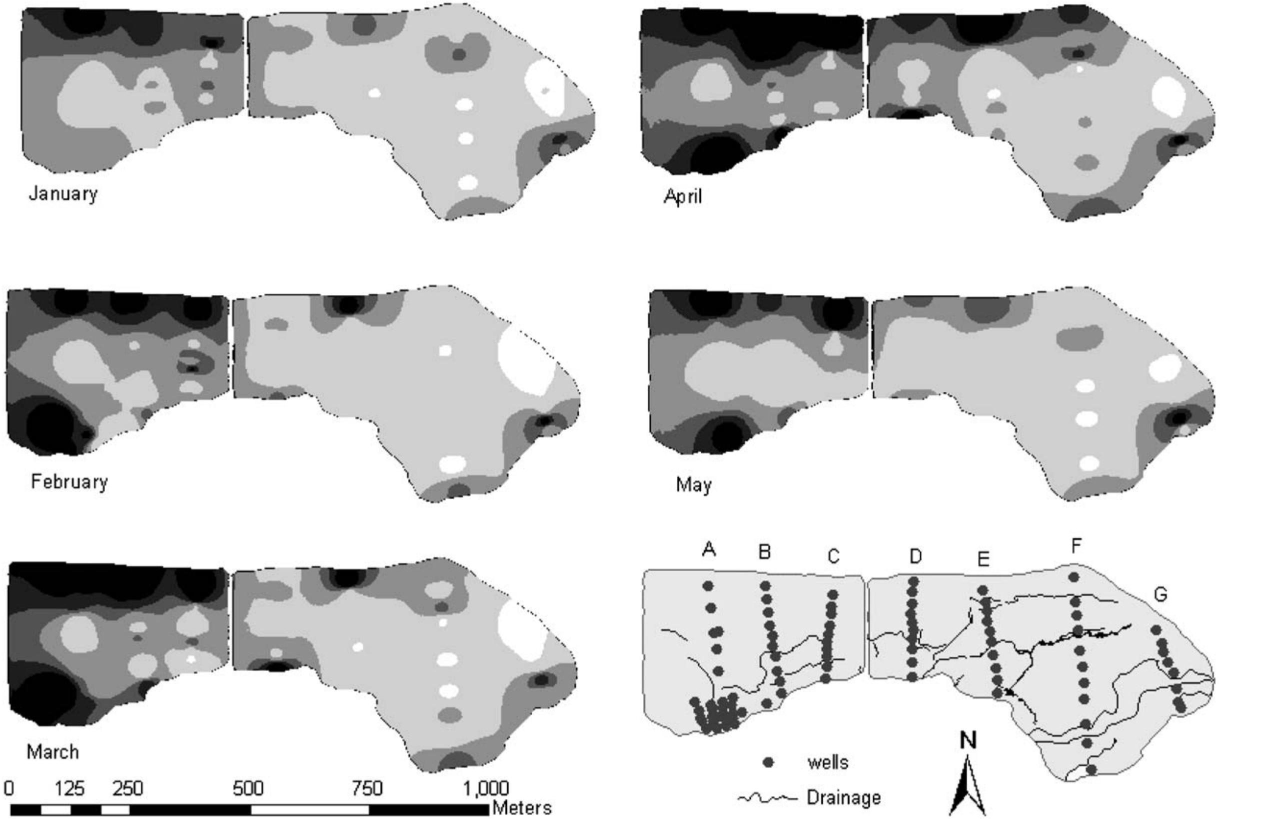

Figure 19.3. Interpolated soil salinity for ten months of 2002 created using the IDW method. The locations of the soil collection sites and transects (A-G) are also presented.

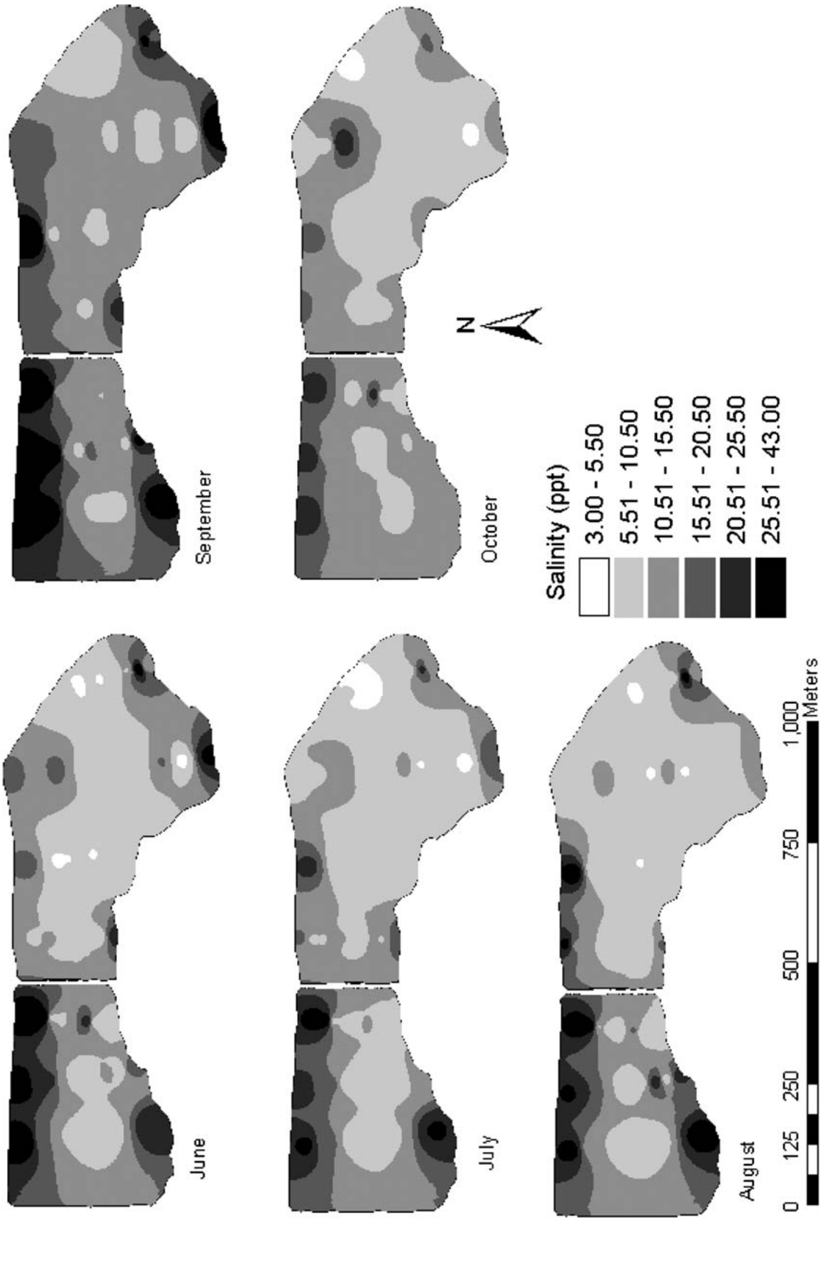

Figure 19.3. (*Continued*)

with a known point and applies them to an unknown point's location (Hurn, 1989; Hurn, 1993; Trimble, 1999; Trimble, 2001). Real-time differential correction involves receiving radio signals to correct the data at the time of collection. It works by receiving GPS differential correction information from local Minimum Shift Keying beacons run by the United States government and transmitting that information to the GeoExplorer III (Trimble, 2001). The beacon used in this study was located in Odessa, Texas, approximately 100 km from the study area.

Using these settings minimized error and allowed attainment of sub-meter horizontal precision on 65% of the 87 observation site locations at a 95% percent level of confidence as calculated by the pathfinder software. The highest calculated error of the horizontal precision estimate was 2.7 m with a mean error of 1.2 m based on the 87 observation site locations.

All of the GPS data collected in the field was imported from the GeoExplorer III into GPS Pathfinder Office software. The data files were then exported as ArcView shapefiles from the GPS Pathfinder Office Software. ArcView 3.3 and ArcGIS 8 were then used to create maps and surfaces that were used to present and/or analyze the collected measurements (ESRI, 1999; Ormsby and Alvi, 1999).

Soil samples from each of the 87 observation sites in the study area were collected on a monthly basis beginning in January 2002 and continuing until October 2002 for 870 total observations. A trowel was used to gather approximately 300 g of surface soil from each observation site. Surface litter was removed and the sample was collected from the top 1 cm of soil (TAES, 1983). When a sampling site was under water, a sample of water was collected. The soil was gathered approximately 2 m from each observation point in a cross pattern. The samples were placed in plastic bags and sealed to prevent evaporation. The sample bags were taken to the University of Texas at San Antonio greenhouse where the soil was analyzed. Soil salinity was measured by making a 1:1 paste (soil:de-ionized water, V:V) (Westerman, 1990; Rowell, 1994). The paste was stirred thoroughly and allowed to sit for 30 min (TAES, 1983). After the 30-min period, the paste was stirred again and measured with a salinity probe. Salinity was measured in parts per thousand. These measurements were then entered into the attribute table of the GIS shapefiles created in ArcView 3.3 and ArcGIS 8 from the collected GPS field sampling site locations.

The soil salinity point measurements were converted to a raster grid to produce a continuous surface or contour plot across the study area. The software creates a raster grid by first dividing the total area into a matrix of equally sized cells (ESRI, 1999; Ormsby and Alvi, 1999; Johnston et al., 2001). Each cell is then assigned a value depending on the method of interpolation used for estimation. In this interpolation, the area was divided into 250 rows and 657 columns for grid cells of approximately 2 m by 2 m. In ArcView 3.3, the Spatial Analyst extension was used to do this interpolation by the IDW method. In ArcGIS 8, the Geostatistical Analyst extension was used to create the surface plots by the kriging method.

Both the IDW and ordinary kriging surface plots were created for the soil salinity measurements for each location and for each of the ten months of the study. Several iterations were performed for each interpolation method using various initial settings of neighborhood size of analysis, lag spacing, and power of magnification. This was performed in a systematic fashion in order to produce the most logical and representative interpolated surface for each method. The settings used for the IDW surface displayed in this study were a neighborhood size of 15 with a power magnification of 3. The settings that produced the best cross-validation error statistics for the ordinary kriging method were for an elliptical search neighborhood with no offset that is divided into four sectors including five points per sector. Both methods allowed for the display and investigation of spatial and temporal trends and patterns of soil salinity levels in the salt marsh. The outputs from the two separate interpolation methods were compared visually as well as by the error statistics produced through cross-validation. The ArcGIS 8.0 software was used to perform cross-validation and generate the mean prediction error and the root-mean-square prediction error.

The monthly soil salinity was also examined for possible significant differences between months using SAS and GraphPad's Prism software packages (Milliken and Johnston, 1992; SAS, 1995, 1999). Bartlett's test was used to test for equal variances (Milliken and Johnston, 1992). In SAS, the Shapiro-Wilk's statistic was used to test for normality (Milliken and Johnston, 1992). The soil salinity data were found in all cases to be non-normal, so transformations were performed to meet the normality assumption. The following transformations were examined in the SAS software; log, reciprocal, square root, exponential, and square. None of the transformations yielded normalized data so nonparametric tests were used. GraphPad's Prism software was used to run the Friedman nonparametric one-way analysis of variance test to account for the repeated measures inherent in the datasets. Dunn's multiple comparison test was used to compare monthly differences.

19.3. Results

The ArcView 3.3 soil surface salinity contour plots created using the IDW method show a range of salinity levels from a low of 3 ppt to a high of

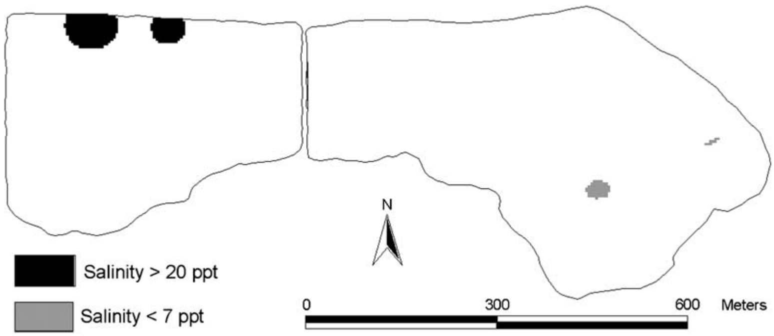

Figure 19.4. Locations of areas where the soil salinity stayed in the identified limit for the entire ten-month study period. The solid black areas are the locations where the salinity level stayed continually high with values always greater than 20 ppt. The light gray colors are consistently low-salinity levels never getting above 7 ppt.

43 ppt (Fig. 19.3). The solid black areas represent the highest salinity levels while lower levels are shown with various patterns. High salinity levels were found along the borders or edges of the study area especially in the northwest with lower salinity levels found toward the center or lower elevations of the marsh associated with the drainage (Fig. 19.3). The surface soils in the eastern half of the study area consistently showed large areas with soil salinity levels in the 3–10 ppt salinity range (Fig. 19.3). There was little variation in the soil salinity levels in these locations through the ten-month study period.

A few locations in the study area had consistently high or low soil salinity (Fig. 19.4). Even though the levels of surface soil salinity maintained a fairly stable pattern on a month-per-month basis, there were months when the levels fluctuated greatly leaving only small areas with constant high or low values for every month. There were two small areas located in the southeastern region of the study area that consistently had soil surface salinity values less than 7 ppt. Surface soil salinity levels greater than 20 ppt were found in locations along the edge of the northwestern part of the study area (Fig. 19.4).

The spatial variation of soil salinity across the study area was examined for each of the seven transects. The seven transects were plotted on separate bar graphs depicting the ten-month soil salinity mean for each location (Fig. 19.5). The nonparametric Kruskal-Wallis test showed significant differences for each transect across the marsh ($P < 0.05$). The trend in the north to south direction across the study area can be most seen with locations at the ends of the transects having significantly higher soil salinity values than areas located in the central region of the study.

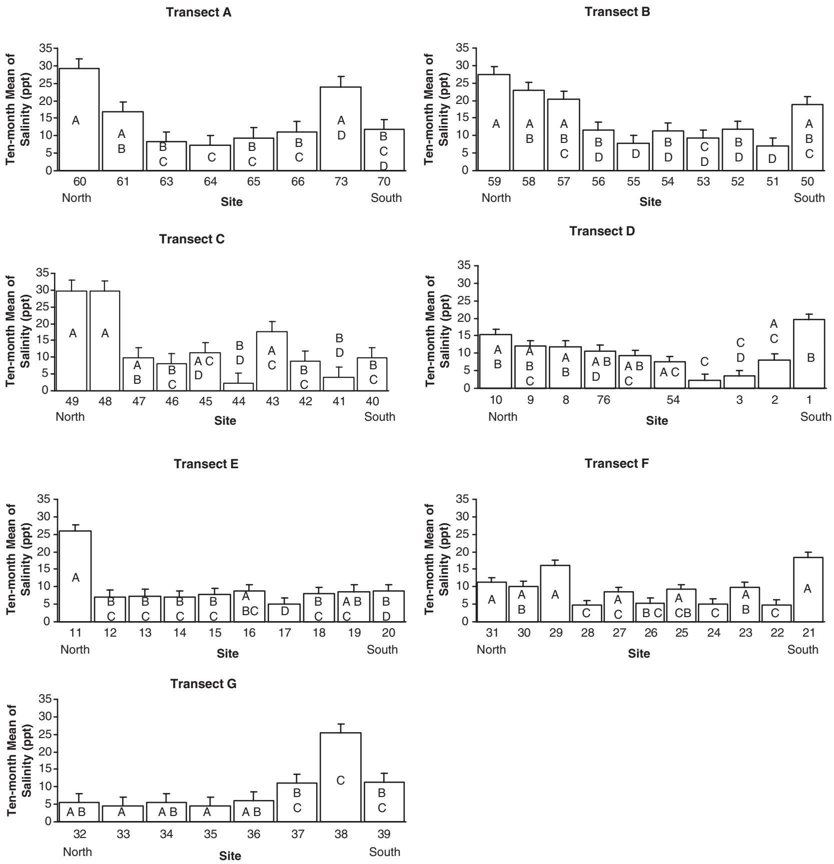

Figure 19.5. Ten-month mean salinity values for the soil-sampling sites located on the seven transect lines across the study area. The bars are the standard errors. The nonparametric Kruskal-Wallis test demonstrated significant differences for each transect ($P<0.05$). Means with the same letter are not significantly different (Dunn's multiple comparison test, $P>0.05$).

These statistically higher soil salinity locations coincided with the high-salinity values displayed in the GIS surface contours (Fig. 19.3).

The monthly means for the salinity data were also plotted for each of the ten months of the study with error bars indicating the 95% confidence interval (Fig. 19.6). The nonparametric Kruskal-Wallis test demonstrated significant differences for each month ($P<0.05$). From January to March, there is only a slight variation in the salinity mean values with 11.10, 11.62, and 12.86 ppt, respectively (Fig. 19.6). April and September were the months with the highest means with September's mean of

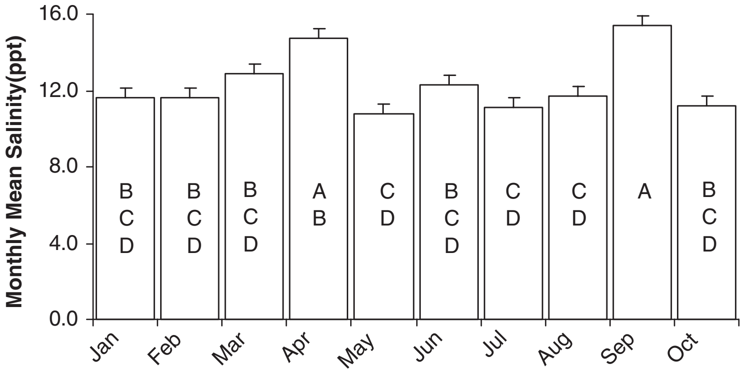

Figure 19.6. Monthly means for the soil salinity data. The mean salinity is presented for each of the ten months in the study period. The nonparametric Kruskal-Wallis test demonstrated significant differences for each transect ($P < 0.05$). The error bar shows the standard error. Means with the same letter are not significantly different between the using Dunn's multiple comparison test ($P > 0.05$).

15.43 ppt being slightly higher than April's 14.72 ppt (Fig. 19.6). May had the lowest mean surface soil salinity with 10.65 ppt. In September, salinity was found to be significantly different from all of the other months except April (Fig. 19.6). For surface soil salinity, April values were significantly different than those for May, July, and August (Fig. 19.6).

The surface contours created using the ordinary kriging method were smoother or less ragged than those created by the IDW procedure (comparing Figs. 19.3 and 19.7). In addition, they also show a large portion of the study area with soil salinity in the range from 5 to 10 ppt (Fig. 19.7). The majority of the higher levels of soil salinity in the range of 25–43 ppt were found along the northwestern border of the study area with occasional occurrences near the southwestern border. February and October show most of the study area with lower levels of salinity with very little area in the higher ranges (Fig. 19.7). April and September show larger areas with higher levels of salinity covering more of the study area than the rest of the time period (Fig. 19.7). The trend shows higher levels always near the borders and lower levels toward the middle of the study area.

Through visual examination both general differences and similarities of the surface plots created using the IDW and ordinary kriging methods could be observed (comparing Figs. 19.3 and 19.7). In the IDW surface plots, the sampling points and transects can more readily be observed (Fig. 3). The ordinary kriging method depicts more gradual and smoother transitions between soil salinity values (Fig. 19.7). The IDW depicts a

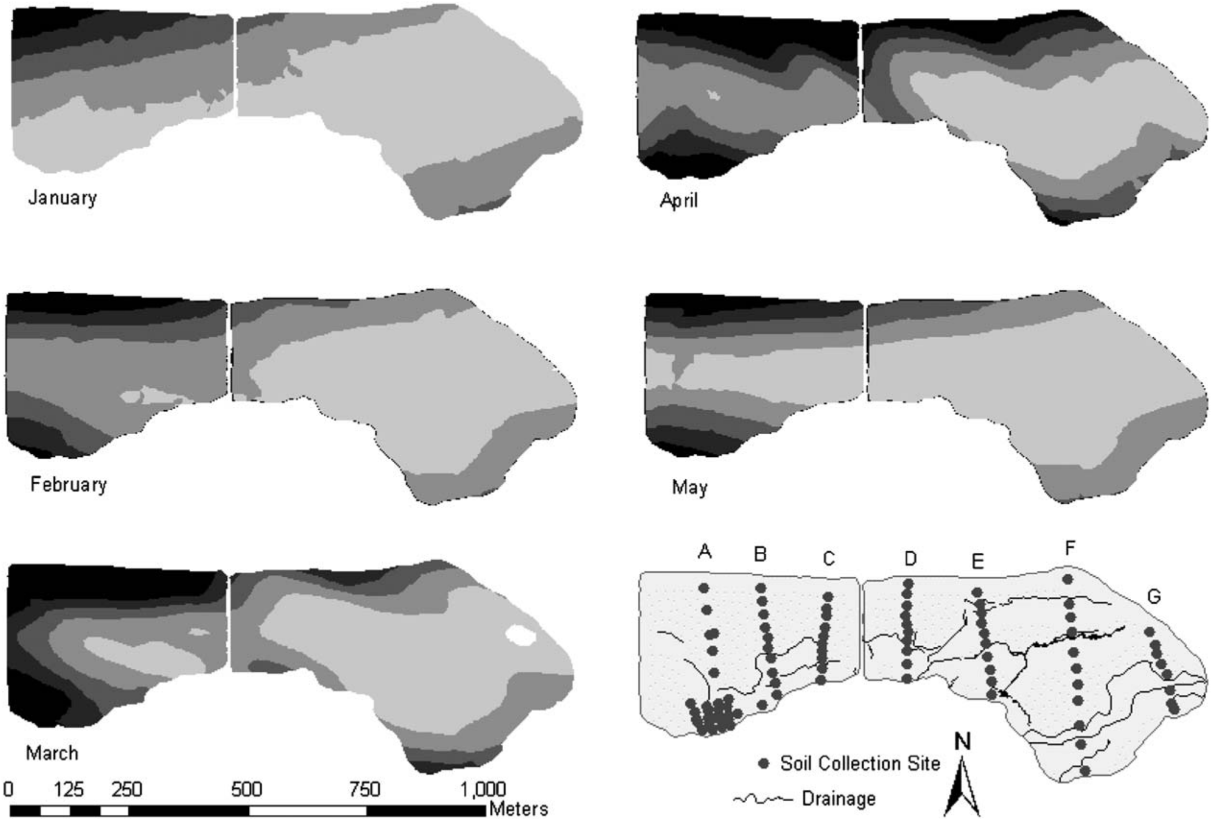

Figure 19.7. Interpolated soil salinity values per ten months of 2002 created using the Ordinary Kriging method in ArcGIS 8.0 software.

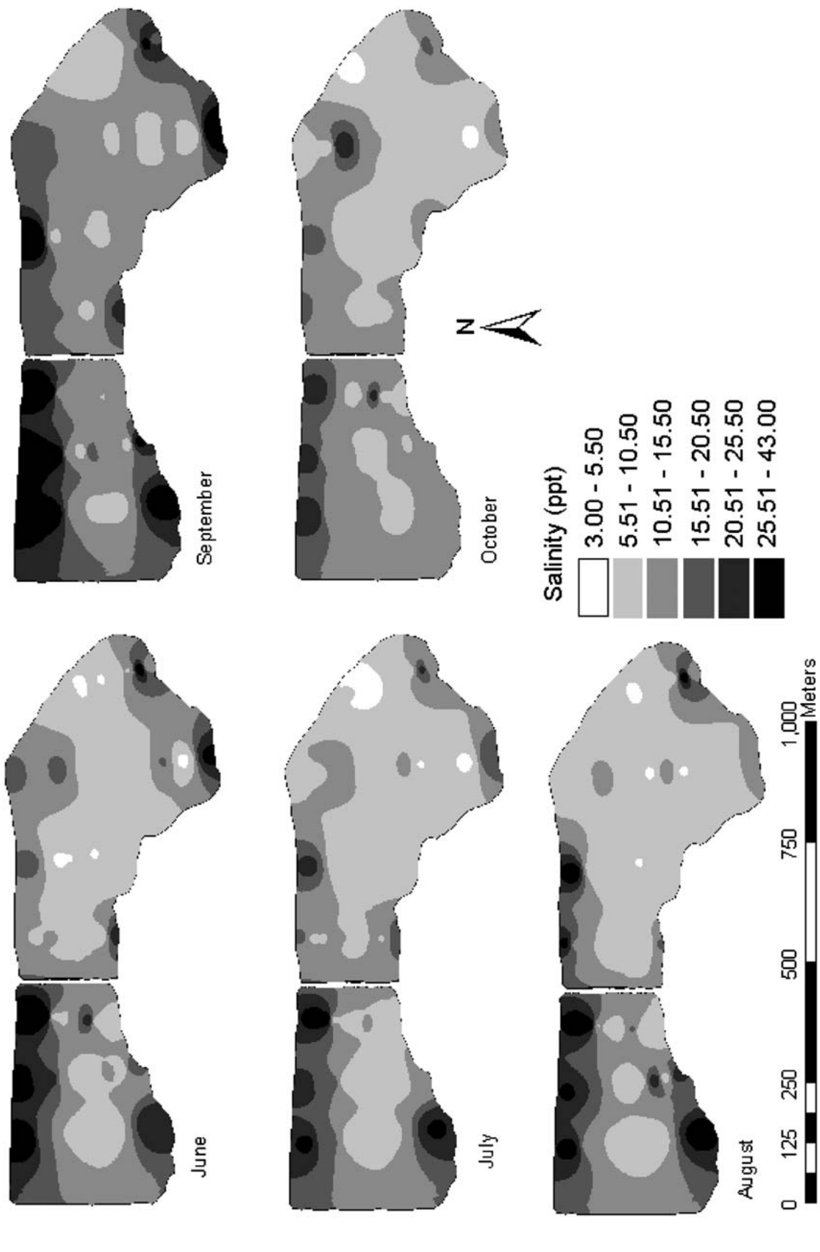

Figure 19.7. *(Continued)*

Table 19.1. Mean and root-mean-square error statistics generated for the interpolated surfaces created using the IDW and ordinary kriging methods. The ordinary kriging method consistently produced values closer to zero indicating it would generally yield a better estimation of the soil salinity

Month	Mean		Root-mean-square	
	IDW	Kriging	IDW	Kriging
January	−0.15	0.05	5.48	5.10
February	−0.69	−0.05	7.31	6.97
March	−1.13	−0.06	7.67	7.30
April	−1.26	−0.29	10.1	8.57
May	−1.02	−0.13	7.63	6.38
June	−1.06	−0.18	8.27	6.59
July	−0.89	−0.36	6.17	5.20
August	−0.87	0.01	7.74	6.07
September	−1.33	−0.27	7.65	6.76
October	−0.46	−0.05	5.97	4.97

larger surface area of the salt marsh covered by the lower values of 3–5 ppt while the ordinary method estimates those same areas to have slightly higher values between 5 and 10 ppt (Figs. 19.3 and 19.7). On the northern border, the IDW method shows localized concentrations of high-soil salinity around the sampling locations while the ordinary kriging method shows a banding pattern in those same areas. The IDW method tends to show less area covered by higher salinity and more area covered with lower salinity while the ordinary kriging method tends to show the reverse. Although both methods of visual representation show similar trends, the ordinary kriging surface contour plots are much smoother (Figs. 19.3 and 19.7).

The IDW and the ordinary kriging methods were evaluated by comparing the overall mean prediction error and root-mean-square prediction error for their surface contour plots (Table 19.1). The ordinary kriging method consistently produced values closer to zero indicating it would generally yield a better estimation of the soil salinity. Both methods depict the northern and southern borders of the salt marsh consistently, with higher levels of soil salinity while the center of the marsh had lower levels.

19.4. Discussion

The surface contour plots available in GIS software provide many new ways to investigate and display diverse results. They facilitate the ability to produce surface contour plots that can estimate and display values across a large surface area from a limited point dataset (Isaaks and Srivastava, 1989; Burrough and McDonnell, 1998). This allows investigators to quickly identify spatial and temporal patterns and trends which they can then examine more critically. These surface plots also allow one the ability to quickly visualize and identify possible interactions and influences that different factors may have in their study area.

The GIS user has numerous interpolation techniques from which to choose depending on the software package selected (Isaaks and Srivastava, 1989; Burrough and McDonnell, 1998; ESRI, 1999; Johnston et al., 2001). Furthermore, variables such as the neighborhood size of analysis, lag spacing, and other settings can be changed within a given interpolation method. The surface contour plots created by these methods may show similar characteristics and trends but will often produce visually dissimilar surface contours with considerable differences at specific locations (Bucher and Vckovski, 1995; Gotway et al., 1996; Brodsky et al., 2001; Dille et al., 2003; Jones et al., 2003; Kravchenko, 2003; Mueller et al., 2004). These dissimilarities are inherent to the mathematical procedures used to create the final surface contour such as the mathematical equations, calculations, and estimations used by those methods (Isaaks and Srivastava, 1989). Some methods are deterministic exact interpolators predicting values at sample locations that are equal to the measured value in the dataset utilized (ESRI, 1999; Johnston et al., 2001). While other methods are geostatistical in their calculations using mathematical models combined with statistical methods to create the final surface contour plots (Johnston et al., 2001). Deterministic interpolators seem to be more sensitive to the distribution and data point value variance entered into the model producing surfaces that are more irregular. While geostatistical interpolation seem to be less sensitive to the distribution and large variances of the point data and consequently produce smoother surface plots.

In this study, both the IDW and the ordinary kriging methods were used to provide examples of different visual outputs created using the same data. The kriging method produced a smooth, more regular interpolated surface, whereas the IDW method produced a surface that was more strongly influenced by local measurements or the values of the specific soil samples in this case (comparing Figs. 19.3 and 19.7). Most likely this was caused by the irregularly spaced pattern of the observation sites that were considerably closer in the west–east direction than the north–south direction. The IDW method produces a fairly exact surface interpolation as long as a regularly distributed sampling pattern is employed (ESRI, 1999; Ormsby and Alvi, 1999; ESRI, 2000; Johnston et al., 2001).

High point value variance or uneven distribution in the sampling patterns often produces sharp peaks or troughs in the output surface (Ormsby and Alvi, 1999; ESRI, 2000; Johnston et al., 2001). The point is that care must be taken with different methods and different settings when creating an interpolated surface in order to avoid interjecting various biases (Gotway et al., 1996; Dille et al., 2003; Jones et al., 2003; Kravchenko, 2003; Mueller et al., 2004). The results can be useful both visually and in predicting values for variables (in this case salinity) between sample points.

When deciding upon the appropriate interpolation method to use to investigate or display data, one must critically evaluate various methods and program settings in order to obtain the best visual representation of logical values between the sample points (Bucher and Vckovski, 1995; Gotway et al., 1996; Brodsky et al., 2001; Dille et al., 2003; Jones et al., 2003; Kravchenko, 2003; Mueller et al., 2004). In the current study, the IDW results are ragged with little smoothing between sampling locations because the IDW method uses exact interpolation with contours formed on the specific measurements entered into the program. Consequently, when the plots are examined it is easy to see where the measurements were actually made. For example, when one examines Fig. 19.3, the locations of the transects (and many soil collection sites) are obvious because of the sharp local differences in the places on the plots and the consequent lack of smoothing. In the kriging method, the northern and southern borders of the salt marsh consistently show the highest levels of soil salinity. These same areas coincide with elevations that are higher than the center of the salt marsh. The higher salinity values at the northern and southern borders of the salt marsh are attributed to a shallow soil or deeper water table that allows the soil to dry and therefore increase the soil surface salt concentration. More of the salts would be washed out of the surface soils in an area with the water table closer to the surface (Neill, 1993; Ala et al., 1995). The areas with high soil salinity can be seen to grow larger as the water table gets deeper and dry areas of the marsh increase in size (see Grunstra, 2002). The same high surface soil salinity areas then recede when the water table rises and the salts are flushed out of the soil by the presence of surface water.

Surface soil salinity in the Diamond Y Spring salt marsh was previously found to be at its lowest level in early spring and increasing during the summer months (Schmidt, 1986; Van Auken and Bush, 1993; Grunstra and Van Auken, 2007; Van Auken and Bush, 1995; Bush, 2006). This fluctuation in surface soil salinity was thought to occur in unison with the cyclic pattern of the water table. A higher water table would allow for more of the salts to be washed out of the surface soils while a lower water table would allow the soil to dry and therefore increase the surface soil salt concentration. A study on the effects of soil salinity on the production of a cool season grass found that spring flooding decreased the soil salinity (Neill, 1993). In another study, high levels of soil water allowed salts to be distributed throughout the soil profile while low levels of soil water caused salt accumulation in the upper soil layers due to the high evaporative rates (Ala et al., 1995).

The expected annual cycle of salinity in the Diamond Y Spring salt marsh was not as apparent as expected due to variation in the annual rainfall pattern (Fig. 19.2) (NCDC, 2002). January of the study year received no precipitation when it usually receives approximately 2 cm while June and July received greater amounts of precipitation than normal (Fig. 19.2). The month of August shows very little precipitation (0.4 cm) compared to the mean precipitation normally expected during that month (5 cm) (Fig. 19.2). Thus, the mean levels for the soil salinity did not show the expected pronounced temporal cyclic pattern. The monthly mean soil salinity fluctuations were observed but they were not as large as expected (Figs. 19.3, 19.6 and 19.7).

The spatial and temporal patterns of abiotic factors and their interactions have been found to play an important role in the distribution of the salt marsh vegetation in many areas and plant communities. Temporal and spatial distributions of soil moisture, pH, and ionic composition were significant in determining plant community locations in a Mediterranean salt marsh (Rogel et al., 2001). Bush (2002, 2006) found that surface salinity had a negative effect on all growth parameters and aboveground dry mass of *Helianthus paradoxus* at the Diamond Y Spring Preserve. In addition, these effects were time dependent. Spatial and temporal fluctuations in three halophyte species in upper coastal salt marsh communities were influenced by saline stress and soil nutrient level (Omer, 2004). Temporal change in soil salt levels was found to determine plant community locations along the shoreline of a desert basin lake (Toft and Elliot-Fisk, 2002). Soil salinity and moisture were also found to effect the spatial and temporal variation in plant germination and establishment in upper tidal marshes of three southern California wetlands (Noe and Zedler, 2001). Plant zonation was related to spatial and temporal variations in soil salinity in southeastern Spain (Ortiz et al., 1995). Vegetation distribution was also determined by soil salinity in spring fed salt marshes in western Utah (Bolen, 1964) and around the Great Salt Lake (Flowers, 1934).

Through the use and application of GIS, greater knowledge of the spatial and seasonal fluctuations of the soil salinity levels in salt marshes can be obtained. GIS interpolations have been used to determine the spatial dynamics of soil salinity in arid and semi-arid conditions (Jordan et al., 2004) as well as to determine the temporal and spatial variability of soil salinity in a coastal saline field (Shi et al., 2005) and a cotton field irrigated with low-quality water (Cetin and Kirda, 2003). In this study, the surface contours created for the Diamond Y Spring salt marsh have identified seasonal fluctuations and spatial distribution in the soil salinity across the salt marsh. The varying soil salinity levels may indicate zonation and probable locations of salt marsh vegetation although this is most likely coupled with the interaction of water level at different points in time during the growing season.

REFERENCES

Ala, F., Ismael, S., Ahmad, R., Shasheen, R., 1995. Effects of salinity and waterlogging on physiological processes and ionic regulation in Atriplex amnícola. Pakistan J. Bot. 27, 283–295.

Bekele, A., Downer, R.G., Wolcott, M.C., Hudnall, W.H., Moore, S.H., 2003. Comparative evaluation of spatial prediction methods in a field experiment for mapping soil potassium. Soil Sci. 168, 15–28.

Bertness, M.D., 1991. Interspecific interactions among high marsh perennials in a New England salt marsh. Ecology 72, 138–148.

Boghici, R., 1997. Hydrogeological Investigations at Diamond Y Springs and Surrounding Area, Pecos County, Texas. M.A. Thesis. University of Texas at Austin, Austin, TX.

Bolen, E.G., 1964. Plant ecology of spring-fed marshes in western Utah. Ecol. Monogr. 34, 143–166.

Borchert, J.R., 1971. The dust bowl in the 1970s. Ann. Assoc. Am. Geogr. 61, 1–22.

Brodsky, L., Vanek, V., Szakova, J., Stipek, K., 2001. Spatial heterogeneity of soil properties. Rost. Vyroba 47, 529–535.

Brune, G.M., 1981. Springs of Texas. Branch-Smith, Inc., Ft. Worth, TX.

Bucher, F., Vckovski, A., 1995. Improving the selection of appropriate spatial interpolation methods. In: Frank, A.U., Werner, K. (Eds.), The Proceedings of the International Conference COSIT '95. Spatial Information Theory: A Theoretical Basis for GIS, Semmering, Austria.

Burrough, P.A., McDonnell, R., 1998. Principles of Geographical Information Systems. Oxford University Press, Oxford, United Kingdom.

Bush, J., 2002. The effects of soil moisture, soil oxygen, and soil salinity on the growth of *Helianthus paradoxus*. Doctoral Dissertation. Department of Environmental Science, The University of Texas at El Paso, El Paso, TX.

Bush, J., 2006. The role of soil moisture, salinity, and oxygen on the growth of *Helianthus paradoxus* (Asteraceae) in an inland salt marsh of west Texas. J. Arid Environ. 64, 22–36.

Bush, J., Van Auken, O.W., 2004. Relative competitive ability of *Helianthus paradoxus* and it progenitors, *H. annus* and *H. petiolaris* (Asteraceae), in varying soil salinities. Int. J. Plant Sci. 165, 303–310.

Cetin, M., Kirda, C., 2003. Spatial and temporal changes of soil salinity in a cotton field irrigated with low-quality water. J. Hydrol. 272, 238–249.

Chapman, V.J., 1974. Salt Marshes and Salt Deserts of the World. Interscience Publishers, Inc., New York, NY.
Dille, J.A., Milner, M., Groeteke, J.J., Mortensen, D.A., Williams, M.M., 2003. How good is your map? A comparison of spatial interpolators. Weed Sci. 51, 44–55.
ESRI, 1999. Getting to Know ArcView GIS. Environmental Systems Research Institute, Redlands, CA.
ESRI, 2000. ArcView Spatial Analyst, An ESRI White Paper. Environmental Systems Research Institute, Redlands, CA.
ESRI, 2003. ArcGIS 8.0 Geostatistical Analyst Extension. Environmental Systems Research Institute, Redlands, CA.
Flowers, S., 1934. Vegetation of the Great Salt lake region. Bot. Gaz. 95, 353–418.
Franzen, D., Peck, A., 1995. Field soil sampling density for variable rate fertilization. J. Prod. Agric. 8, 568–574.
Freund, H., Petersen, J., Pott, R., 2003. Investigations on recent and subfossil salt marsh vegetation of the East Frisian barrier islands in the southern North Sea (Germany). Phytocoenologia 33, 349–375.
Gotway, C.A., Ferguson, R.B., Hergert, G.W., Peterson, T.A., 1996. Comparison of kriging and inverse-distance methods for mapping soil parameters. Soil Sci. Soc. Am. J. 60, 1237–1247.
Grunstra, M.B., 2002. Spatial and temporal hydrogeological description and ecological community comparison of the Diamond Y Spring Preserve. M.S. Thesis. Department of Earth and Environmental Science, University of Texas at San Antonio, San Antonio, TX.
Grunstra, M.B., Van Auken, O.W., 2007. Factors that influence the distribution and cover of *Helianthus paradoxus* in a west Texas salt marsh. Phytologia 89, 24–42.
Hart, D., 2002. Description and comparison of the upland plant communities of the Diamond Y Spring Preserve. M.S. Thesis. Department of Biology, University of Texas at San Antonio, San Antonio, TX.
Higinbotham, C.B., Alber, M., Chalmers, G., 2004. Analysis of tidal marsh vegetation pattern in two Georgia estuaries using aerial photography and GIS. Estuaries 27, 670–683.
Hurn, J., 1993. Differential GPS Explained. Trimble Navigation Limited, Sunnyvale, CA.
Hurn, J., 1989. GPS A Guide to the Next Utility. Trimble Navigation Limited, Sunnyvale, CA.
Isaaks, E.H., Srivastava, R.H., 1989. Appl. Geostatistics. Oxford University Press, New York, NY.
Johnston, K., Ver Hoef, J.M., Krivoruchko, K., Lucas, N., 2001. Using ArcGIS Geostatistical Analyst. ESRI Inc., Redlands, CA.
Jones, N.L., Davis, R.J., Sabbah, W., 2003. A comparison of three-dimensional interpolation techniques for plume characterization. Ground Water 41, 411–419.
Jordan, M.M., Navarro-Pedreno, J., Garcia-Sanchez, E., Mateu, J., Juan, P., 2004. Spatial dynamics under arid and semi-arid conditions: Geological and environmental implications. Environ. Geol. 45, 448–456.
Kravchenko, A., 2003. Influence of spatial structure of accuracy of interpolation methods. Soil Sci. Soc. Am. J. 67, 1564–1571.
Kravchenko, A., Bullock, D.G., 1999. A comparative study of interpolation techniques for mapping soil properties. Agronomics J. 91, 393–400.
Lam, N., 1983. Spatial interpolation methods: A review. Am. Cartographer 10, 129–149.
Larkin, T.J., Bomar, G.W., 1983. Climatic Atlas of Texas. Texas Department of Water Resources, LP-192, Austin, TX.

Laslett, G.M., McBratney, A.B., Pahl, P.J., Hutchinson, M.F., 1987. Comparison of several spatial prediction methods for soil pH. J. Soil Sci. 38, 325–341.

Lavelle, P., Spain, A.V., 2001. Soil Ecology. Kluwer Academic Publishers, Dordrecht, The Netherlands.

Lefohn, A.S., Knudsen, H.P., Logan, J.L., Simpson, J., Bhumralkar, C., 1987. An evaluation of the kriging method to predict 7-h seasonal mean ozone concentrations for estimating crop losses. J. Air Pollut. Control Assoc. 37, 595–602.

McDonald, C., 1999. Endangered and threatened wildlife and plants; determining the status for the plant *Helianthus paradoxus* (Pecos sunflower). Fed. Register 64, 56582–56590.

Milliken, G.A., Johnston, D.E., 1992. Analysis of Messy Data. Chapman & Hall/CRC, Boca Raton, FL.

Mueller, T.G., Pierce, F.J., Schabenberger, O., Warncke, D.D., 2001. Map quality for site specific fertility management. Soil Sci. Soc. Am. J. 65, 1547–1558.

Mueller, T.G., Pusuluri, N.B., Mathius, K.K., Cornelius, P.L., 2004. Map quality for ordinary kriging and inverse distance weight interpolation. Soil Sci. Soc. Am. J. 68, 2042–2047.

National Climatic Data Center, 2002. National Oceanic and Atmospheric Administration. U.S. Department of Commerce, Washington, DC.

Neill, C., 1993. Seasonal flooding, soil salinity and primary production in northern prairie marshes. Oecologia 95, 499–505.

Niering, W.A., Warren, R.S., 1980. Vegetational patterns and processes in New England salt marshes. BioScience 30, 301–307.

Noe, G.B., Zedler, J.B., 2001. Spatio-temporal variation of salt marsh seedling establishment in relation to the abiotic and biotic environment. J. Veg. Sci. 12, 61–74.

Odum, W.E., 1988. Comparative ecology of tidal freshwater and salt marshes. Annu. Rev. Ecol. Syst. 19, 147–176.

Omer, L., 2004. Small-scale resource heterogeneity among halophytic plant species in an upper salt marsh community. Aquat. Bot. 78, 337–448.

Ormsby, T., Alvi, J., 1999. Extending Arcview GIS. Environmental Systems Research Institute, Redlands, CA.

Ortiz, R., Rogel, J.A., Alcaraz, F., 1995. Soil-vegetation in 2 coastal salt marshes in southeastern Spain. Arid Soil Res. Rehab. 9, 481–493.

Phillips, D.L., Lee, E.H., Herstrom, A.A., Hogsett, W.E., Tingley, D.T., 1997. Use of auxiliary data for spatial interpolation of ozone exposure on southeastern forests. Environmetrics 8, 43–61.

Rives, J.L., 1980. Soil Survey of Pecos County, Texas. United States Department of Agriculture Soil Conservation Service, Washington, DC.

Robinson, T.P., Metternicht, G., 2005. Comparing the performance of techniques to improve the quality of yield maps. Agr. Syst. 85, 19–41.

Rogel, J.A., Silla, R.O., Ariza, F.A., 2001. Edaphic characterization and soil ionic composition influencing plant zonation in a semiarid Mediterranean salt marsh. Geoderma 99, 81–98.

Rowell, D., 1994. Soil Science: Methods and Applications. Longman Group UK Limited, Essex, England.

SAS Institute, 1999. The Analyst Application, first ed. SAS Institute Inc., Cary, NC.

SAS Institute., 1995. Logistic Regression Examples Using the SAS System, Version 6, first ed. SAS Institute Inc., Cary, NC.

Schmidt, R.H.J., 1986. Chihuahuan Climate. In: Barlow, J.C., Powell, A.M., Timmermann, B.N. (Eds.), Invited papers from the Second Symposium on the Resources of the Chihuahuan Desert Region. Chihuahuan Desert Research Institute, Fort Davis, TX, pp. 40–63.

Schoeneberger, P.J., Wysocki, D.A., Benham, E.C., Broderson, W.D., 1998. Field book for describing and sampling soils. Natural Resources Conservation Services, USDA, National Soil Survey Center, Lincoln, NE.

Shi, Z., Li, Y., Wang, R., Makeshine, F., 2005. Assessment of temporal and spatial variability of soil salinity in a coastal saline field. Environ. Geol. 48, 171–178.

Small, T.A., Ozuna, G.B., 1993. Ground-water conditions in Pecos County, Texas. USGS Water-Resources Investigations, Report 92-4190.

T.A.E.S., 1983. Soil Analysis Texas Agriculture Extension Service. College Station, TX.

T.P.W.D., 2003. Wetland Ecology. Texas Parks and Wildlife Department, Austin, TX.

Toft, C., Elliot-Fisk, D., 2002. Patterns of vegetation along a spatiotemporal gradient on shoreline strands of a basin desert lake. Plant Ecol. 158, 21–39.

Trimble, 1999. GeoExplorer 3, Operations Manual. Trimble Navigation Limited, Sunnyvale, CA.

Trimble, 2001. GPS Mapping for GIS with GeoExplorer 3, Classroom Manual. Trimble Navigation Limited, Sunnyvale, CA.

Ungar, I.A., 1974. Inland halophytes of the United States. In: Reinhold, R.J., Queen, W.H. (Eds.), Ecology of Halophytes. Academic Press, New York, NY, pp. 235–306.

USGS., 2002. U.S. Geological Survey. Ground Water Atlas of the United States. Oklahoma, TX. HA 730-E.

Van Auken, O.W., Bush, J.K., 1993. Annual Report. The Nature Conservancy of Texas. San Antonio, TX.

Van Auken, O.W., Bush, J.K., 1995. Annual Report. The Nature Conservancy of Texas. San Antonio, TX.

Van Auken, O.W., Bush, J.K., 1998. Spatial relationships of *Helianthus paradoxus* (Compositae) and associated salt marsh plants. Southwest. Nat. 43, 313–320.

Van Auken, O.W., Grunstra, M.B., Brown, S.C., 2007. Composition and structure of a west Texas salt marsh. Madroño. (In press).

Veni, G., 1991. Delineation and preliminary hydrogeologic investigations of the Diamond Y Spring, Pecos County, Texas Report to the Nature Conservancy of Texas.

Warrick, A.W., Zhang, R., El-Harris, M.K., Myers, D.E., 1988. Direct comparisons between kriging and other interpolators. In: Wierenga, P.J., Bachelet, D. (Eds.), Validation of Flow and Transport Models for the Unsaturated Zone. Proceedings. New Mexico State University, Las Cruces, NM.

Weisz, R., Fleischer, S., Smilowitz, Z., 1995. Map generation in high-value horticultural integrated pest management: Appropriate interpolation methods for site-specific pest management of Colorado potato beetle (Coleoptera: Chrysomelidae). J. Econ. Entomol. 88, 1650–1657.

Westerman, R.L., 1990. Soil Testing and Plant Analysis, third ed.. Soil Science Society of America, Inc., Madison, WI.

Wollenhaupt, N.C., Wolkowski, R.P., Clayton, M.K., 1994. Mapping soil test phosphorus and potassium for variable-rate fertilizer application. J. Prod. Agric. 7, 441–448.

Zimmerman, D., Pavlik, C., Ruggles, A., Armstrong, M.P., 1999. An experimental comparison of ordinary and universal kriging and inverse distance weighting. Math. Geol. 31, 375–390.